

1Research paper published in *Remote Sensing of Environment*

2<https://doi.org/10.1016/j.rse.2019.01.013>

3© 2019. This manuscript version is made available under the CC-BY-NC-ND 4.0 license

4<http://creativecommons.org/licenses/by-nc-nd/4.0/>

5

6**Continuous monitoring of land change activities and post-disturbance dynamics from**

7**Landsat time series: a test methodology for REDD+ reporting**

8

9P. Arevalo*, P. Olofsson and C.E. Woodcock.

10Department of Earth & Environment, Boston University, 685 Commonwealth Avenue, Boston,

11MA 02215, USA

12

13*Corresponding author. Email: parevalo@bu.edu

14

15Keywords: time series, Colombian Amazon, land cover, deforestation, Landsat, IPCC, estimation

16Abstract.

17The REDD+ mechanism of UNFCCC was established to reduce greenhouse gases emissions by
18means of financial incentives. Of importance to the success of REDD+ and similar initiatives is
19the provision of credible evidence of reductions in the extent of land change activities that
20release carbon to the atmosphere (e.g. deforestation). The criteria for reporting land change areas
21and associated emissions within REDD+ stipulate the use of sampling-based approaches, which
22allow for unbiased estimation and uncertainty quantification. But for economic compensation for
23emission reductions to be feasible, agreements between participating countries and donors often
24require reporting every year or every second year. With the rates of land change typically being
25very small relative to the total study area, sampling-based approaches for estimation of annual or
26bi-annual areas have proven problematic, especially when comparing area estimates over time. In
27this paper, we present a methodology for monitoring and estimating areas of land change activity
28at high temporal resolution that is compliant with international guidelines. The methodology is
29based on a break detection algorithm applied to time series of Landsat data in the Colombian
30Amazon between 2001 and 2016. A biannual stratified sampling approach was implemented to
31(1) remove the bias introduced by the change detection and classification algorithm in mapped
32areas derived from pixel-counting; and (2) provide confidence intervals for area estimates
33obtained from the reference data collected for the sample. Our results show that estimating the
34area of land change, like deforestation, at annual or bi-annual resolution is inherently challenging
35and associated with high degrees of uncertainty. We found that better precision was achieved if
36independent sample datasets of reference observations were collected for each time interval for
37which area estimates are required. The alternative of selecting one sample of continuous
38reference observations analyzed for inference of area for each time interval did not yield area

estimates significantly different from zero. Also, when large stable land covers (primary forest in this case, occupying almost 90% of the study area) are present in the study area in combination with small rates of land change activity, the impact of omission errors in the map used for stratifying the study area will be substantial and potentially detrimental to usefulness of land change studies. The introduction of a buffer stratum around areas of mapped land change reduced the uncertainty in area estimates by up to 98%. Results indicate that the Colombian Amazon has experienced a small but steady decrease in primary forest due to establishment of pastures, with forest-to-pasture conversion reaching 103 ± 30 kha (95% confidence interval) in the period between 2013 to 2015, corresponding to 0.22% of the study area. Around 29 ± 17 kha (95% CI) of pastureland that had been abandoned shortly after establishment reverted to secondary forest within the same period. Other gains of secondary forest from more permanent pastures averaged about 12 ± 11 kha (95% CI) , while losses of secondary forest averaged 20 ± 12 kha (95% CI).

521. Introduction

53Current tropical deforestation has been estimated to account for 7-14% of the annual CO₂
54emissions released into the atmosphere by human activities whereas intact tropical primary
55forests sequester an equal amount (Achard et al., 2014; Goetz et al., 2015; Harris et al., 2012;
56Houghton et al., 2012). However, recent research suggests that a reduction in carbon density of
57tropical primary forest due to disturbance exceeds the emissions from deforestation, with the
58result that tropical forests are becoming a net source of carbon to the atmosphere (Baccini et al.,
592017). The need for a reduction of emissions is thus more urgent than ever. Efforts to reduce
60global deforestation have led to the establishment of international frameworks like the United
61Nations Programme on Reducing Emissions from Deforestation and Forest Degradation (UN-
62REDD, 2016) that stipulate financial incentives to countries for reducing carbon emissions from
63tropical deforestation and forest degradation. For such frameworks to be successful, robust
64approaches that provide estimates of carbon emissions and removals with proper uncertainty
65metrics are required (IPCC, 2003). Methods to estimate carbon emissions and removals in the
66tropics typically rely on a gain/loss approach in which emission factors (i.e. carbon content per
67unit area per land cover type) and area of land change activities (i.e. areal extent of human
68activities that cause emission or removal of carbon such as deforestation, also called activity
69data) are multiplied (GFOI, 2016). Depending on the quantity of information required, and the
70degree of analytical complexity, the Intergovernmental Panel on Climate Change (IPCC)
71guidelines classifies the methodological approaches into three different Tiers: Tier 1, or the
72“default method”, relies on default emission factors data while Tier 2 requires country-specific
73emission factors; at Tier 3, higher-order methods typically include models and data that address
74national circumstances, and pixel- or stand-level tracking of land change activity over time

75(IPCC, 2003; GFOI, 2016). For representation of land areas and changes in area and condition,
76the IPCC identifies three approaches: Approach 1 does not include any direct data on land
77activities but simply country-scale area estimates of land categories at different times; Approach
782 requires a land change matrix, but without a spatial representation of the change; while
79Approach 3 requires a spatially and temporally explicit representation of land categories and
80conversions (GFOI, 2016). Following the Cancun Agreement of the United Nations Framework
81Convention on Climate Change (UNFCCC), countries that wish to report carbon emissions and
82removals under the requirements of IPCC guidelines need to create a system for Measurement,
83Reporting and Verification (MRV) for communication of the mitigation procedures and
84estimation approaches (UNFCCC, 2018). The national MRV system includes approaches for
85national forest monitoring in accordance with the IPCC Tier system (IPCC, 2006).

86 While tropical deforestation and associated carbon emissions have been extensively
87studied during the last three decades (Achard et al., 2002; Baccini et al., 2012; Brown, 1997;
88DeFries et al., 2002; FAO, 1993; Hansen et al., 2013), the last couple of years have witnessed
89remarkable developments in environmental remote sensing. The opening of the Landsat archive
90in 2008 (Woodcock et al., 2008) has allowed for production of global maps of forest cover
91change (Hansen et al., 2013; Kim, 2010) and time series analysis of satellite data to study
92changes on the land surface (see for example Kennedy et al., 2010; Verbesselt et al., 2010; Zhu
93and Woodcock, 2014). New missions with global acquisition strategies and free data policies are
94already in orbit (Sentinel-2A, -2B and Landsat-8) and more are forthcoming (Landsat-9, -10 and
95Sentinel-2C, -2D). In addition, statistical protocols for unbiased estimation of area have become
96an integral part of forest and land cover monitoring (McRoberts, 2011; Olofsson et al., 2013;
97Stehman, 2013). Together, these advancements enable a more comprehensive analysis of land

98change that meets the highest requirements of IPCC for land representation. Still, there are
99relatively few studies in the scientific literature focused on the use of these methods for
100advancing operational forest monitoring in MRV systems. Notable exceptions are the Guyana
101MRV system that conforms to the IPCC Approach 3 for multiple land cover classes (GFOI,
1022016); the national forest monitoring system of Peru that employs Landsat-based time series
103analysis and unbiased estimation of forest cover change (Potapov et al., 2014); the PRODES
104system of Brazil (Instituto Nacional de Pesquisas Espaciais (INPE), 2016) based on manual
105interpretation of Landsat imagery; and the Mexican MAD-MEX system (Gebhardt et al., 2014)
106that uses time-series analysis, segmentation and approaches for statistical inference. Colombia
107has experienced an increase in forest monitoring capacity with a Government agency (Instituto
108de Hidrología, Meteorología y Estudios Ambientales, IDEAM) dedicated to the establishment of
109a forest monitoring system (IDEAM, 2016). The Colombian system is built upon good practices
110in remote sensing and sampling-based estimation, including stratified estimation and
111implementation of new algorithms that make use of the Landsat archive. The aforementioned
112forest monitoring systems are impressive and have provided valuable information on the state of
113tropical forests. Still, what is missing is a system that tracks the conversions between the six
114IPCC land categories, including the dynamics of post-disturbance landscapes, at high temporal
115and spatial resolution, coupled with unbiased estimation protocols for provision of biannual
116estimates of activity data.

117 In this paper we test a methodology for continuous monitoring and estimation of areas of
118land cover and land change that is compliant with IPCC Approach 3 for representation of land.
119The methodology builds on recent advancements in the field of environmental remote sensing,
120using algorithms for time series analysis (Zhu and Woodcock, 2014a) and estimation protocols

121(Olofsson et al., 2014; Stehman, 2013). The performance of the methodology is tested for the
122Colombian Amazon between 2001 and 2016.

1232. Study area

124The study area corresponds to the Colombian Amazon region as defined by the Sinchi Amazonic
125Institute of Scientific Research (*Instituto Amazónico de Investigaciones Científicas*) (Figure 1).
126The area, which is mostly covered by tropical rainforest, makes up more than two thirds of the
127forest area of Colombia (Galindo et al. IDEAM, 2014). The Colombian Amazon contains
128substantial carbon stocks and is one of the most biodiverse regions in the world (Asner et al.,
1292012; Duivenvoorden, 1996; Olson and Dinerstein, 2002; Orme et al., 2005).

130 While no regional maps of the dynamics and patterns of conversion between multiple
131land categories over time are being produced in Colombia, a few studies have attempted to
132identify general patterns of land use. Sánchez-Cuervo et al. (2012) documented vegetation
133recovery in the Andes and a significant loss of woody vegetation in the northern boundary of the
134Amazon region between 2001 and 2010. Sy et al. (2015) attributed smallholder crop and mixed
135agriculture as the main drivers of deforestation, and underlined the importance of other wooded
136lands in the process. These are important findings that highlight the relevance of monitoring
137secondary forests and the fate of the post-disturbance landscape. Armenteras et al. (2006) and
138Etter et al. (2006b) identified colonizing agriculture (*colonización agrícola*) in the Colombian
139Amazon, characterized by pasture establishment and cattle ranching along the deforestation
140frontier as the main cause of ecosystem change in the region. Etter et al. (2006a) found that areas
141that experienced deforestation were partially offset by regenerating vegetation between 1999 and
1422002, which was further corroborated by Aide et al. (2013), again, emphasizing the separation of
143primary and secondary forest, and the monitoring of post-disturbance landscapes. These

practices increase the forest fragmentation and make land cover patterns more “patchy”, spontaneous and unplanned than those documented in the neighboring countries of Brazil and Ecuador (Armenteras et al., 2006). This, combined with the fact that the rate of deforestation is less than in Brazil and Ecuador (FAO, 2010), makes the Colombian Amazon a complex but relevant landscape to test the presented methodology.

149



150

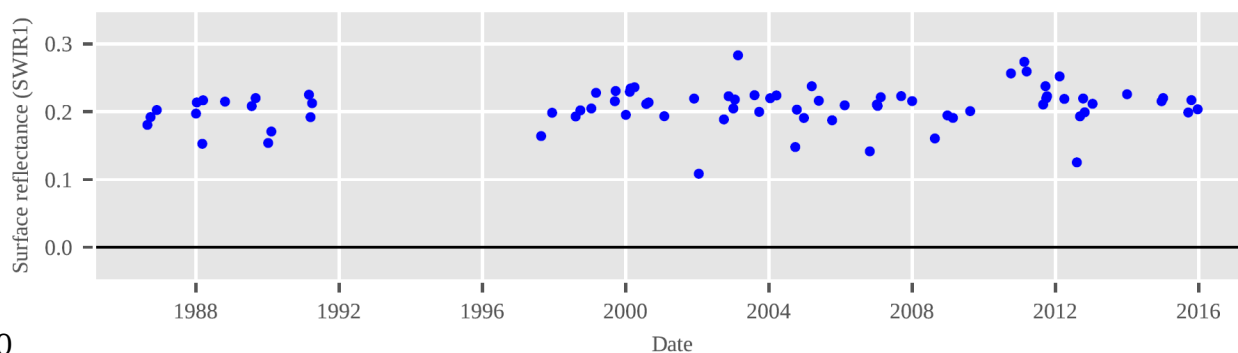
Figure 1. Study area and Landsat scenes processed. The Landsat WRS-2 path and row are displayed for each scene. The total area of study region is 46,822 kha.

1513. Methodology

1523.1 Time series analysis of land conversion

153 All available terrain-corrected (L1T), surface reflectance images from the TM, ETM+, and OLI
154 sensors onboard Landsat-5, -7 and -8 with a cloud cover of less than 80% were downloaded from
155 the EROS Center Science Processing Architecture (ESPA) website (USGS, 2010) for the 25
156 Landsat path and rows covering the study area (Figure 1). Because of a data gap around the mid-
157 1990s (Figure 2), only data acquired after 1997 were used. This yielded a total of 5,184 images
158 that were stacked chronologically to create time series of surface reflectance.

159



160

Figure 2. Time series of short-wave infrared observations (the SWIR1 band) acquired by Landsat
-5, 7 and -8 of a pasture in the Colombian Amazon. A clear gap in available observations can be
seen between 1992 and 1997. Landsat WRS-2 path 7, row 59; coordinates 73.9290 W, 1.9687 N.

161

162 A Python implementation of the Continuous Change Detection and Classification

163 (CCDC) algorithm was applied to each Landsat pixel in each of the 25 Landsat path and rows

164 from 1997 to 2016. CCDC (and YATSM, the Python implementation used in this study) searches

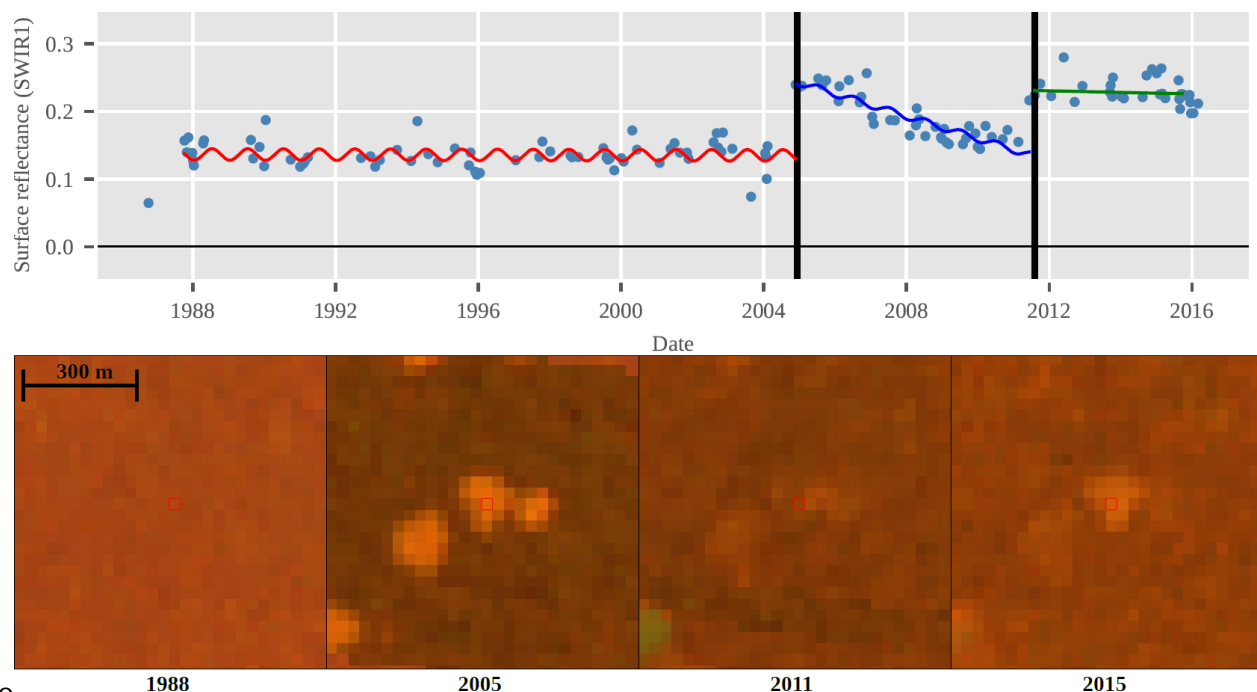
165 for “breaks” in a time series by monitoring for change in the residuals of the forecast from

166statistical models (Holden, 2016a; Zhu et al., 2012; Zhu and Woodcock, 2014a). The models
167predict the surface reflectance for any given date, and if the difference between observed and
168predicted reflectance across multiple bands is sustained for a certain number of consecutive
169observations, a change is flagged by the algorithm. After a change is detected, this process is
170repeated for the remaining observations in the time series iteratively. The time segments are
171subsequently classified in a supervised manner using a random forest classifier (Breiman, 2001)
172with time series model coefficients as input features, and training data. This approach enables
173identification of land categories before and after land change activities are detected. Two
174masking procedures were applied to reduce the number of cloudy observations in the data. The
175first procedure filters cloudy observations as flagged by Fmask (Zhu and Woodcock, 2012). The
176second procedure uses two multi-temporal methods similar to the Tmask procedure (Zhu and
177Woodcock, 2014b) that search for noise and remove it during the model-fitting phase.

178 Of importance to the stated objectives is the ability of the algorithm to track post-
179disturbance landscape dynamics; an example is provided in Figure 3 which shows a pixel located
180along the deforestation frontier of the Colombian Amazon. Figure 3 shows an example of
181colonizing agriculture which is common along the deforestation frontier: *Primary Forest*,
182present from the start of the time series, is converted to *Pasture* in 2005 which in turn is
183abandoned a year or two after its creation and *Secondary Forest* is allowed to regenerate. The
184regeneration is evident by the decreasing trend in the time series of shortwave infrared
185reflectance, but in 2011, the regenerated forest is again converted to *Pasture* which appears to be
186the prevailing land use until the end of the time series. The situation in Figure 3 is a rather
187common example of the landscape dynamics in the region. It is included to showcase the ability
188of the algorithm to detect the activities on the land surface including the timing, and importantly,

189to identify the condition of post-disturbance landscapes. It is important because: 1) these
 190dynamics have a profound impact on the terrestrial carbon budget and will, if not identified
 191correctly, result in erroneous estimates of carbon emissions and removals; and 2) many current
 192forest monitoring systems in the tropics are limited to mapping and estimating forest loss and
 193gain (Espejo and Jonckheere, 2017) without the ability to provide a complete picture of the
 194landscape dynamics. An underlying hypothesis of the presented research is that CCDC, as
 195illustrated in Figure 3, will be able to map land conversions and post-disturbance landscapes
 196across the study area such that the resulting map data can be used to stratify the landscape in a
 197way that allows for sufficiently precise estimation of activity data at annual or bi-annual
 198frequency.

199



200

Figure 3. Time series of observations of SWIR1 surface reflectance measured by Landsat TM, ETM+, OLI band 5 (blue dots; upper) and snippets of Landsat composites in NIR-SWIR1-RED

band combination (lower). CCDC predictions of surface reflectance are plotted as solid lines and detected breaks as vertical black lines. (Landsat path-row 6-59, pixel coordinates: 72.1795 W, 1.4725 N).

201

202 Given the low density of satellite data in the study area, only simplified time series
203models could be used for change detection. The time series models included one harmonic to
204account for annual variability, which is the only major seasonal fluctuation observed in this area.
205The Red Near- and Infrared bands were used to detect changes in the time series. The time series
206segments were required to have at least nine valid observations, and five consecutive
207observations were required to flag a change when the prediction differed from the observed.
208Training data were collected manually over ten Landsat paths and rows to account for the natural
209variability in each of the land categories, particularly in the *Forest* category. Training data were
210identified using Landsat imagery and the TSTools plugin for QGIS (Holden, 2016b; QGIS
211Development Team, 2009). In total, 420 training polygons were collected, with the total number
212of training pixels per land category being approximately proportional to the mapped area of the
213category, based on initial test maps produced and refined iteratively. Training data were obtained
214for the six IPCC land categories: *Forest*, *Grassland*, *Urban*, *Pastures/Crops*, *Water* and *Other*
215(mostly river sandbanks and rocky surfaces), plus a seventh category: *Secondary Forest*. The
216term *Secondary Forest* is used for the remainder of the manuscript to describe vegetation that
217exhibited a clear temporal pattern of regeneration but without having fully recovered to the state
218of a primary forest. It should be noted that even though we use the term “secondary”, the forest
219might have been disturbed more than once. *Grassland* and *Pasture* were defined as separate map
220classes because the former is mostly natural while the latter is the result of direct human

intervention and the most common post-deforestation land category. An additional map class denominated *All-classes-to-unclassified* was assigned for pixels where the time series presented a break with a labeled segment prior to it, but no segment fitted afterwards. Training polygons labeled *Forest* were mostly collected in areas where the presence of stable primary forest with a closed homogenous canopy forest was evident and thus required no formal definition. This decision was corroborated by looking at the individual pixel time series, which displayed a stable, flat trend centered on surface reflectance around 0.15 in the Landsat SWIR1 band, as seen in Figure 5. Polygons labeled *Secondary Forest* were collected using a similar approach, only selecting pixels with segments that showed a clear negative slope with reflectance around 0.20 in the SWIR1 band following a disturbance event. A single classifier created from the training dataset across the study area was applied to the time series segments for creation of land cover annual maps from 2001 to 2016 for each Landsat scene. This allowed for an initial training and stabilization period between the start of the time series in 1997 and the beginning of the analysis to find change, in 2001. Annual maps were mosaicked in sequential order from low to high WRS-2 path and row number (i.e. north to south, east to west), discarding the relatively small overlap zones of each previous scene in order to simplify the process.

3.2 Area estimation

Areas retrieved by pixel-counting in maps will be incorrect because of classification errors. Therefore, areas and their confidence intervals need to be estimated by applying unbiased estimators to sample data of reference observations of land surface conditions (GFOI, 2016; Olofsson et al., 2013; Stehman, 2000). A sample-based approach to area estimation is emphasized by the IPCC Good Practice Guidelines for reporting within the UNFCCC treaty (IPCC, 2003, preface; GFOI 2014, p. 25): “inventories for the land use, land-use change and

244forestry sector that are neither over- nor underestimates so far as can be judged, and in which
245uncertainties are reduced as far as practicable”. In statistical terms, the first criterion is related to
246*bias*; an estimator is characterized as unbiased if it produces a parameter estimate such that the
247mean value taken over all possible samples is equal to the population parameter (Cochran 1977).
248Still, if several random samples are selected, the estimates obtained from each of the samples
249will be different because of the randomization of the selection, even if using an unbiased
250estimator. This uncertainty is characterized by construction of a confidence interval, which
251relates to the second IPCC criterion.

252 In this study, a stratified design and estimation approach (Cochran, 1977; Olofsson et al.,
2532013) were implemented. Stratified random sampling was chosen to target the sampling of areas
254exhibiting land change activity, which as informed by the maps, were a very small proportion of
255the study area. Further, the stratified estimator has proven efficient when applied to categorical
256observations (GFOI, 2016). The stratification contained six stable land strata and five land
257change strata representing mapped land dynamics between 2001 and 2016 (Table 1). The *All-*
258*classes-to-unclassified* class was included in the stratification, but its area was not estimated. A
259buffer stratum corresponding to mapped forest in close proximity (< 90 m) to mapped transitions
260from *Forest-to-Pasture* was added to the stratification and used as a part of the sampling design
261to diminish the impact of omission errors. The buffer stratum was added because the *Forest*
262stratum occupied 86% of the study area, and any pixels in this stratum identified in the reference
263classification as exhibiting land change activity (i.e. omission errors of change activities in the
264map) will carry a large area weight and dramatically reduce the precision in area estimates of
265land change activities.

266 The total sample size was determined using the stratified variance estimator solved for n
267as described in Cochran (1977) with a target standard error of 0.3% (equivalent of 1.6 Mha, or a
26895% confidence interval of ± 3.1 Mha) of the *Forest-to-Pasture* class, which had a mapped area
269of 0.87% (4.5 Mha) of the total area between 2001 and 2016. In other words, the sample size was
270selected to achieve a margin of error of 60% if using the stratum area as an indication of the area
271estimate. While a margin of error (defined here as the half width of the 95% confidence interval
272divided by the estimate) of 60% seems high, it must be recognized that estimating an area that is
273assumed to be less than one percent of the study area is inherently difficult. For example,
274targeting a margin of error of 25% would have resulted in a sample size of almost 6,000
275sampling units. Hence, the motivation behind these numbers was mainly practical and a
276compromise between precision and available human resources. Targeting a 60% margin of error
277gave a total sample size of 1,050 sample units that were allocated to strata following “good
278practices” for estimation of area of change (Olofsson et al., 2014): 50 and 75 units were allocated
279to the smaller strata and the remaining 400 units were allocated to the larger *Forest* stratum. The
280sampling assessment unit was a 30 m \times 30 m Landsat pixel, which was chosen to coincide with
281the minimum mapping unit.

282 A reference observation was provided for each unit in the sample by examining a time
283series of Landsat observations of surface reflectance using the TSTools plugin for QGIS
284(Holden, 2016b; QGIS Development Team, 2009). Examples of pixels labeled as forest in the
285reference sample can be seen in Figure 5. The legend of reference observations (Table 1) was
286based on the stratification legend to facilitate estimation of area, and was recorded along with
287time of change (if any). Multi-temporal very-high resolution imagery was used if available, and
288the following measures were taken to increase the interpretation confidence: the interpreters were

carefully trained to understand and identify the land dynamics in the region; strata information was not made available to the interpreter during the collection of reference observations; and the reference label was assigned one of three levels of confidence. Labels with the lowest confidence, or labels on which interpreters disagreed, were double-checked at a later stage and modified. A stratified estimator was applied to the sample data for estimation of area with 95% confidence intervals following Olofsson et al. (2013). To assess the effectiveness of the buffer stratum to contain omission errors, areas with 95% confidence intervals were also estimated without using the buffer stratum (i.e. by combining the *buffer* and *Stable Forest* map classes and using the resulting class as the *Forest* stratum in the calculations). An overview of this workflow can be seen in Figure 4.

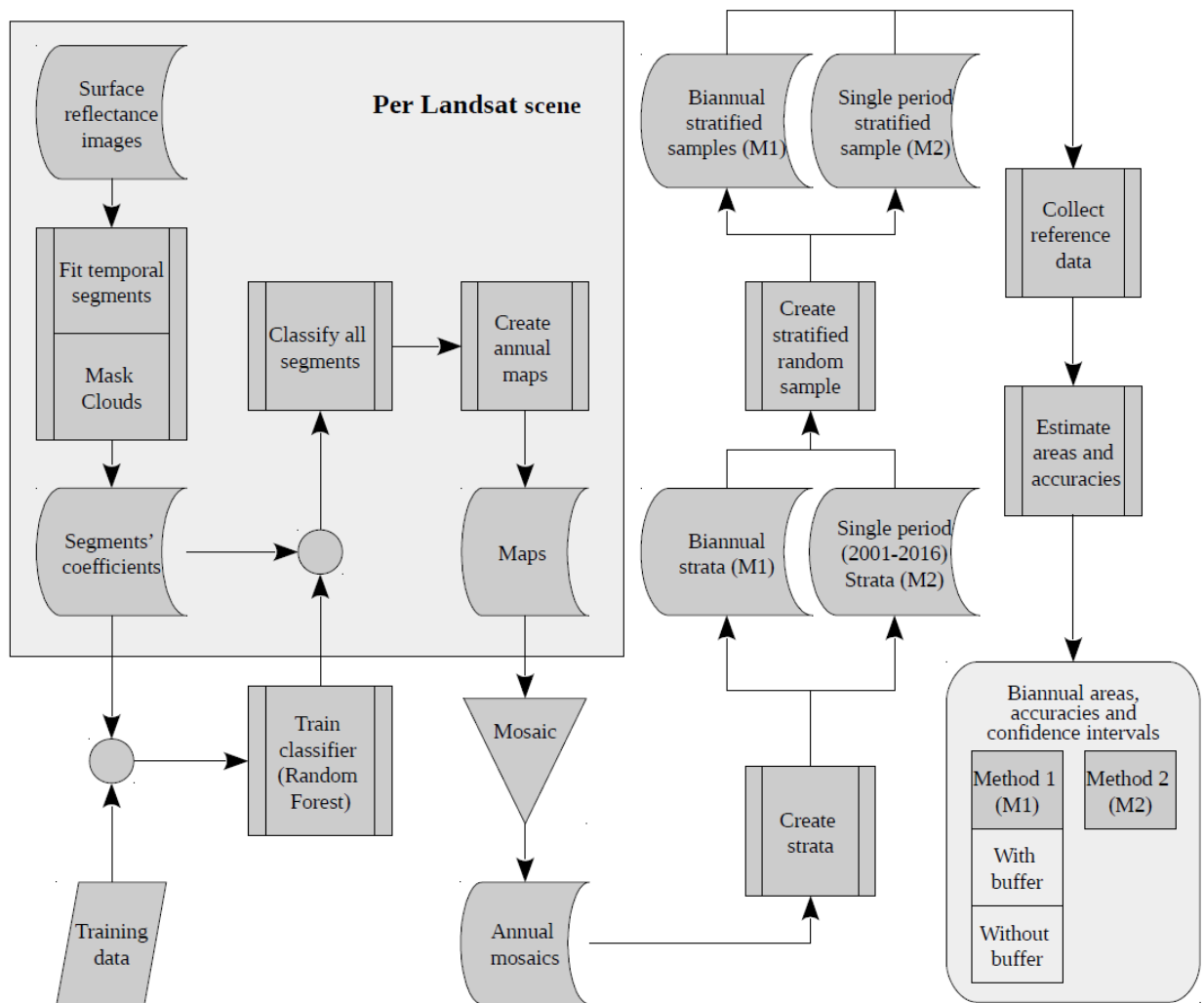


Figure 4. Overview of the workflow used to estimate areas, accuracies and uncertainty using maps created from time series of Landsat imagery as a source of stratification and manually collected reference data.

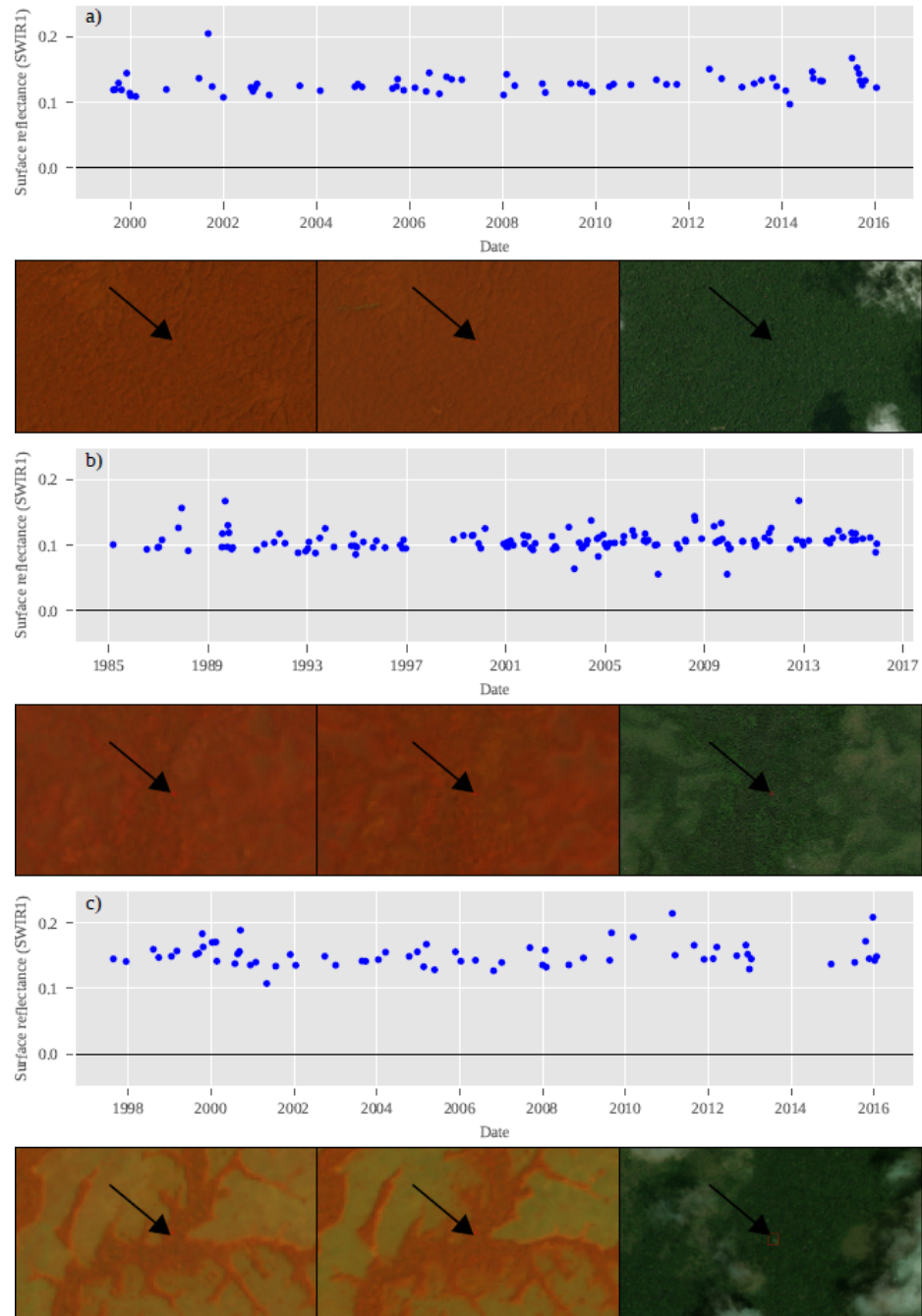


Figure 5. Examples of stable forest in time series of Landsat SWIR1 surface reflectance for a pixel in a) an area of intact primary forest, b) the edge between forest and shrublands and c) a riparian forest next to natural grasslands. Landsat subsets in RGB NIR-SWIR1-RED band combination are shown for dates near the beginning and end of the time series, respectively.

High-resolution imagery (zoomed) of the example pixels from Bing Maps are shown to the right of the Landsat images.

Table 1. Strata names and their description, strata weight (W_h [%]) based on the map of stable and change classes between 2001-2016, and number of sample units allocated to strata (n_h). The areas of the All-classes-to-unclassified and Buffer strata were not estimated. The term “stable” implies the presence of a single land cover class during the entire period being analyzed.

Stratum name	Description	W_h	n_h
Stable forest	Stable forest.	85.70	400
Stable grassland	Stable natural grassland.	2.81	75
Stable Urban + Stable other	Areas that show stable urban cover, as well as other bright surfaces like exposed rock and sand.	0.08	50
Stable pasture-cropland	Stable human introduced pasturelands and croplands.	4.91	75
Stable secondary forest	Areas that show sustained vegetation regrowth over the course of two years or more.	1.06	50
Stable water	Stable water bodies.	1.29	50
Forest to pasture	Areas that experienced conversion from forest to pastures or croplands.	1.40	50
Forest to secondary forest	Areas that experienced a brief conversion to pastures or croplands that were abandoned shortly thereafter and display a regrowing trend.	0.26	50
Gain of secondary forest	Areas that experienced a conversion from pastures, grasslands, urban, water and other to secondary forest.	0.11	50
Loss of secondary forest	Areas of secondary forest that were converted to any other class (except to forest).	0.23	50
Other to other	Other transitions that are not relevant.	0.45	50
All to unclassified	Areas of classes other than forest and secondary forest that experienced a disturbance but have no class label afterwards.	0.35	50
Buffer	Areas of stable forest that were assigned to a 'buffer' stratum surrounding the <i>Forest to pasture</i> stratum.	1.37	50

302

303 Central to reporting of trends in carbon emissions and removals from land surface

304activities is the ability to provide estimates at high temporal frequency. The UNFCCC requires

305reporting at annual or bi-annual time intervals (GFOI, 2016), which complicates the estimation

306of land change activities as the areas are often very small at such short intervals. In this study, the
307most common activity was the conversion of forest to pastures, which was mapped as occupying
3080.87% of the study area over 16 years. At annual intervals, the area of this activity would average
309less than a tenth of a percent. Even at a bi-annual intervals, the area will be small from an
310estimation perspective. The situation of estimating small areas in the presence of large strata of
311stable land cover is a complicated issue in many national forest monitoring systems aimed
312providing area estimates of land change activity data for reporting within the REDD+
313mechanism (Espejo and Jonckheere, 2017).

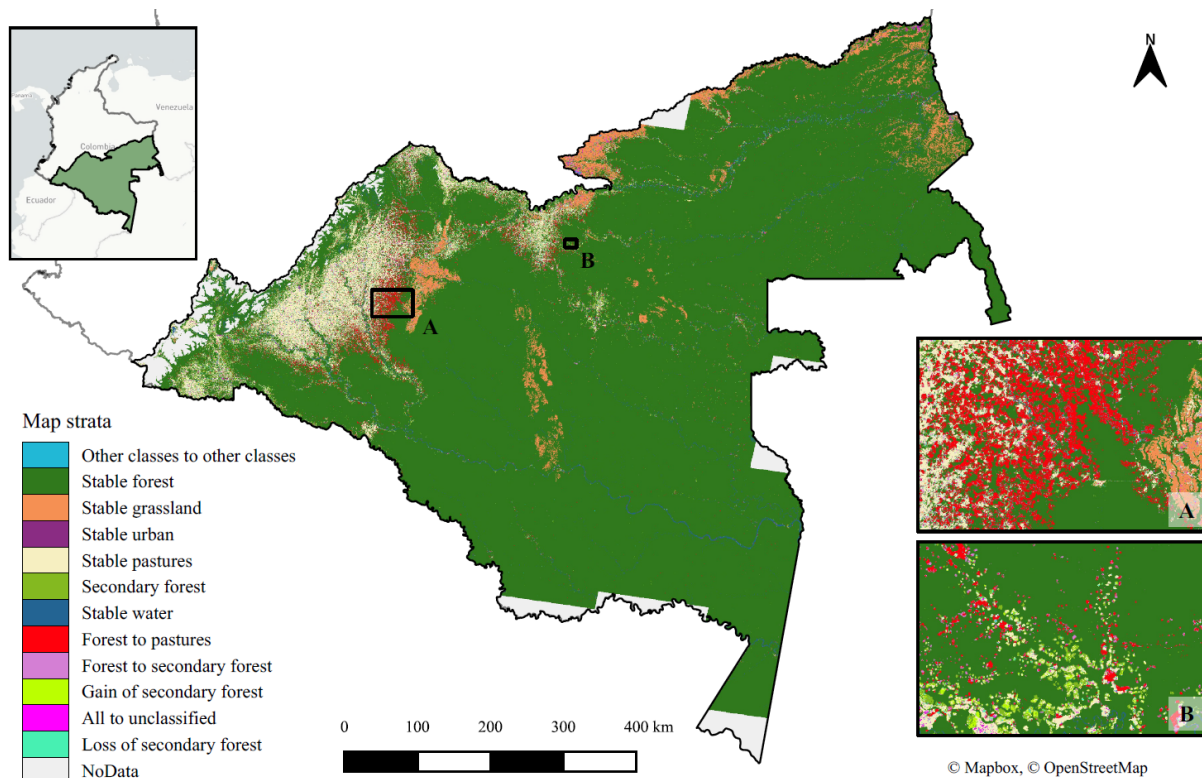
314 To explore solutions and to provide better guidance on this issue, two approaches were
315investigated for area estimation. The first approach uses only one sample for all sixteen years of
316the study period that is analyzed such that area estimates are obtained for bi-annual intervals. The
317analysis is based on the construction of a ratio estimator and indicator functions as described in
318Stehman (2014); code and documentation are provided in a GitHub repository
319<https://github.com/parevalo/workflow>. While this approach requires only a single sample, it
320requires continuous reference observations for the entire 2001-2016 time period at each sample
321location. We introduce the term “continuous reference observations” to distinguish from
322observations at only one point in time or at shorter time interval. In this case, the reference
323observations were collected in biannual intervals. The second approach is based on the selection
324of a sample for each time interval for which area estimates are required; for bi-annual reporting,
325seven independent samples were required and obtained from each biannual strata map (annual
326reporting would have required fifteen samples which we did not have the resources to provide).
327Stratified estimators were constructed for each sample such that independent estimates were
328provided for each two-year period. We selected seven samples of equal size and allocation by

329stratified random sampling using the design described above (i.e. 1,050 units allocated to the
330study area according to the recommendations in Olofsson et al. (2014) and shown in detail in
331Appendix 2). We hypothesize that the single-sample-approach will save time and cost as the
332collection of sample data is often a time-consuming process but result in less precise estimates.
333We hypothesize a lesser precision because the stratification of the study area is based on the
334change map 2001-2016, which makes strata are less likely to correspond to the targeted land
335change activities at any given bi-annual interval. The result is an increased likelihood of having
336very few, or even zero, reference observations of land change activities (*Forest-to-Pasture* for
337example) for certain bi-annual intervals, especially in the beginning of the study period. Whether
338estimates obtained using the single-sample-approach have similar or better precision than those
339obtained from the multiple-samples-approach (i.e. smaller standard errors), and whether the
340single-sample-approach results in such large uncertainty that independent samples are required
341for each time interval, were key questions to be answered in this research.

3424. Results

343The products generated in this study were: (i) a map of land categories and conversions for the
344time period 2001-2016 (Figure 6); (ii) annual map products of the IPCC land categories and
345biannual maps of stable categories and their conversions; and (iii) biannual area estimates with
34695% confidence intervals of activity data, i.e. the IPCC land categories of the most prevalent
347activities involving conversions to and from *Forest*, *Secondary Forest* and *Pasture*.

348



349

350 Figure 6. Map of IPCC land categories including conversions between 2001 and 2016 detailing:
 351 A) areas of conversion from forest to pasture, and B) areas with evidence of secondary forest and
 352 heterogeneous land changes.

353

354 Central to this study are the bi-annual area estimates with 95% confidence intervals of
 355 stable land categories and conversions shown in Figure 7. As expected, it was found that the
 356 multiple-samples-approach of collecting sample data that represented each time interval yielded
 357 more precise estimates than the single-sample-approach (Figure 7, Appendix 1 and 3). With the
 358 single-sample-approach, several bi-annual area estimates of land change activities were highly
 359 uncertain and at times not significantly different from zero (Appendix 1 and 3). The margins of
 360 error, calculated as the half width of the 95% confidence interval divided by the area estimate
 361 (Figure 8 and Appendix 3), were in general smaller with the multiple-samples-approach for the

362 area estimates of the land change activities. Although a few individual area estimates were not
363 significantly different from zero even with bi-annual sample data, the precision of estimates was
364 considerably higher and sufficient to construct temporal trajectories of the more important and
365 prevalent activities, including Forest-to-Pasture and Forest-to-Secondary Forest. Note however
366 that even with the multiple-samples-approach, the Forest-to-Pasture estimate for 2003-2005 was
367 highly uncertain and the 2001-2003 and 2009-2011 periods were not significantly different from
368 zero.

369 The use of a buffer stratum was highly effective at diminishing the impact of omissions
370 of observed deforestation activities present in the *Forest* stratum. For example, the standard error
371 of the bi-annual area estimates of Forest-to-Pasture decreased between 54% and 98%. The effect
372 on other land change activities, which were also substantial with the exception of *Gain-of-*
373 *Secondary-Forest*, can be seen in Table 2. Note the use of a buffer stratum does not decrease the
374 precision in area estimates.

375

Table 2. Comparison of standard error of areas in kha per period for the change strata, with and without the buffer stratum.

Period	Forest to pasture		Forest to sec. forest		Gain of sec. forest		Loss of sec. forest	
	No buffer	Buffer	No buffer	Buffer	No buffer	Buffer	No buffer	Buffer
2001 - 2003	316	104	184	104	0.8	0.8	11.8	11.8
2003 - 2005	355	53	36	36	12.3	12.3	0.5	0.5
2005 - 2007	327	7	130	4	1.3	1.3	12.8	12.8
2007 - 2009	272	10	241	8	49.2	49.2	92.6	13.7
2009 - 2011	223	103	159	15	36.4	36.4	98.4	36.7
2011 - 2013	285	10	157	6	2.7	2.7	2.3	2.3
2013 - 2015	255	15	128	9	5.6	5.6	6.3	6.3

376

377

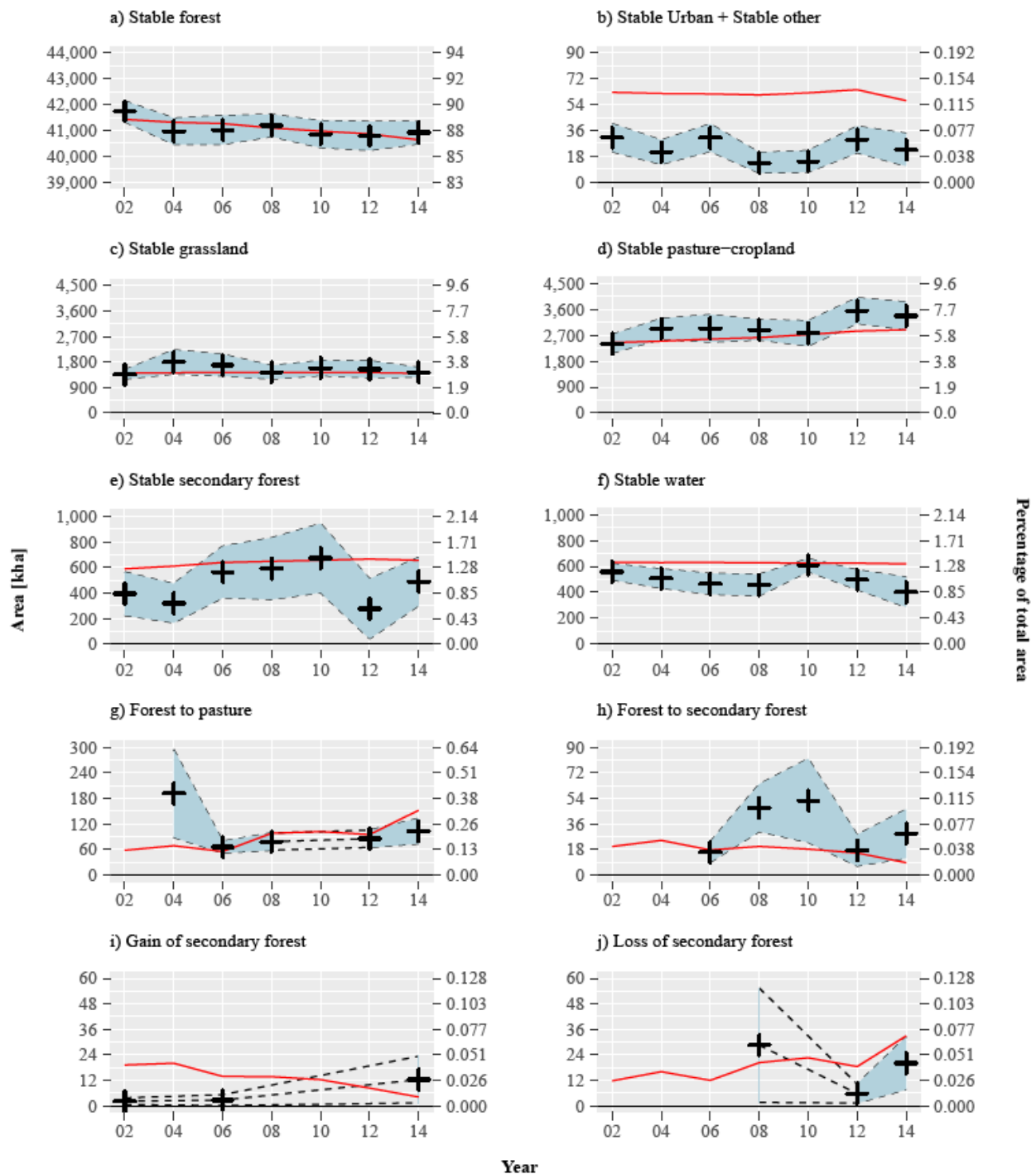


Figure 7. Bi-annual area estimates with 95% confidence intervals (dashed lines) for stable and change classes, estimated from the reference data using the multiple-samples-approach. Cross markers represent values that are statistically different from zero (i.e. confidence interval does

not include zero). The red continuous line represent areas obtained directly from the map by pixel-counting. The years on the x-axes represent the middle of each bi-annual period for visualization purposes (02 for 2002, 04 for 2004 and so on). The y-axes were set to aid in the visualization of the areas (but kept similar in rows where the same scale was sensible) given the large differences in magnitude. The panel for the *Other-to-other* class was removed, as it did not contain any relevant information.

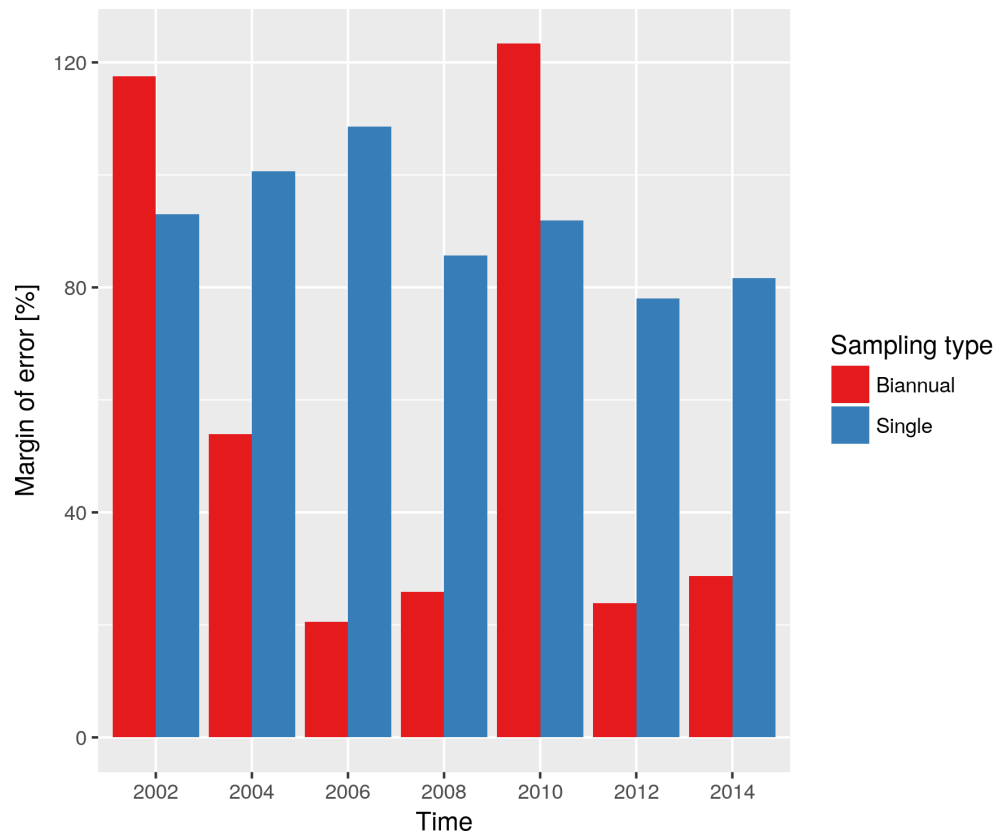


Figure 8. Comparison of margins of error of the bi-annual *Forest-to-Pasture* area estimates obtained by multiple-samples-approach (with the *Buffer* stratum) and single-sample-approach.

380 The overall accuracy of the map 2001-2016 was 94.1% ($\pm 0.81\%$). Class-specific
381 accuracies of biannual area estimates were highly variable (Table 3 and Table 4). Not
382 surprisingly, higher accuracies were obtained for larger map classes including stable land
383 categories and lower accuracies for the change classes.

Table 3. User's accuracy for each class and period, in percentage.

	2001-2003	2003-2005	2005-2007	2007-2009	2009-2011	2011-2013	2013-2015
Other to other	4	0	0	4	0	4	4
Stable forest	99	98	98	99	98	98	99
Stable grassland	87	91	89	89	92	92	91
Stable Urban + Stable other	42	32	44	22	20	42	24
Stable pasture-cropland	81	89	84	92	81	95	85
Stable secondary forest	30	24	42	58	54	12	38
Stable water	86	78	72	68	92	76	56
Forest to pasture	62	64	58	38	38	48	40
Forest to secondary forest	50	28	34	52	58	24	22
Gain of secondary forest	4	4	2	10	6	2	2
Loss of secondary forest	8	6	22	28	20	8	18

Table 4. Producer's accuracy for each class and period, in percentage.

	2001-2003	2003-2005	2005-2007	2007-2009	2009-2011	2011-2013	2013-2015
Other to other	100	0	0	98		22	100
Stable forest	99	99	99	99	99	98	98
Stable grassland	90	72	76	89	83	85	88
Stable Urban + Stable other	85	95	87	99	86	91	60
Stable pasture-cropland	83	76	73	83	80	76	73
Stable secondary forest	45	46	48	64	53	29	51
Stable water	97	97	98	94	94	96	86
Forest to pasture	21	23	49	48	24	54	59
Forest to secondary forest	8	11	37	22	20	22	7
Gain of secondary forest	36	6	10	2	2	3	1
Loss of secondary forest	7	100	16	20	9	26	29

386

3875. Discussion

388 The analysis provided evidence of a small but steady decline in primary forest driven by
389 conversion to pasture. Although subtle and low, the rate of this conversion was estimated to have

390increased during the period (excluding the very uncertain area estimate for 2003-2005). Overall,
391these results are consistent with the official national estimates of forest cover loss (Cabrera et al.,
3922011) and with the spatial patterns of land cover change reported in previous studies (Armenteras
393et al., 2006; Etter et al., 2006b, 2006a). To properly model the carbon emissions and removals,
394estimating the rate of primary forest to pasture is important but not sufficient – the fate of the
395post-disturbance landscape will determine if, when, and how the carbon emitted by the forest
396conversion activity is offset by secondary activities such abandonment and forest regeneration
397that remove atmospheric carbon. We found that the area of primary forest that was converted to
398pasture, but that reverted back to forest during the study period (i.e. *Forest-to-Secondary-*
399*Forest*), never reached above 60 kha per period -- in comparison, the area estimates of *Forest-to-*
400*Pasture* were never below 60 kha per period. If treating the conversion of forest to pastures as
401“forest loss” and not accounting for the post-disturbance dynamics involving pasture
402abandonment and secondary forest regeneration, the implications of land change activities on
403terrestrial carbon dynamics would be mischaracterized.

404 Along with the establishment of pasture, illicit cropland is an important driver of
405deforestation in the Colombian Amazon. According to Government statistics, coca plantations
406affect a much smaller area than forest to pasture conversion in the Colombian Amazon
407(UNODC, 2016) but our observations indicate that coca plantations are more likely to be
408abandoned. Pasture and coca were not separated but the latter was included in the pasture
409category. The decision to not distinguish coca from pasture was driven by the focus of this study
410on the mapping and estimation of IPCC land categories -- both coca and pasture were considered
411as belonging to the IPCC *Cropland* category (GFOI, 2016) -- and because of the similarity in
412spectral signature between coca and pasture. However, because of the observed difference in the

413post-disturbance dynamics between coca and pasture, an article exploring the drivers and
414patterns of the land change dynamics in the region is currently in preparation in which separate
415area estimates are provided for coca and pasture.

416 In addition to the dynamics of conversion between forest and pasture, individual rates of
417gain and loss of *Secondary Forest* were monitored and estimated. These dynamics are typically a
418result of conversion from pastures to secondary forest, and vice versa. Except for a dip from
4192010 to 2012, the combined effect of *Secondary Forest* dynamics resulted in a stable area of
420*Secondary Forest* without any obvious trend throughout the study period (Figure 7, h-j).

4215.1 *Comparison of sampling approaches*

422Of importance to this study and future potential applications of the presented methods is the
423estimation protocol. While maps are essential for stratifying the study area to guide the sampling,
424the results communicated to decision makers within frameworks and treaties such as REDD+
425and UNFCCC are not obtained directly from maps but estimated from sample data. As explained
426earlier, even the most sophisticated classification approach will not generate map products that
427are free of errors, which necessitates a sampling-based approach to area estimation. The
428importance of sampling-based estimation in a remote sensing context has been explained and
429illustrated in several articles (e.g. McRoberts, 2011; Olofsson et al., 2014; Stehman, 2013) and
430international guidance documents (GFOI, 2016, 2014), but few studies have explored methods
431for providing a time series of estimates. A notable exception is Cohen et al. (2016), who
432provided annual estimates of forest disturbance across the U.S. by two-stage cluster sampling
433with primary sampling units stratified by forest area. Also, Potapov et al. (2017) presented
434annual area estimates of forest cover loss in Bangladesh using a single sample with continuous
435reference observations. Because international treaties and climate negotiations require annual or

bi-annual reporting (GFOI, 2016), the topic of estimating areas at high temporal frequency will need further exploration by the remote sensing community. The collection of sample data is often an arduous task and approaches that relieve practitioners of the burden of collecting such data are needed. Therefore, we tested a single-sample-approach similar to that of Cohen et al. (2016) and Potapov et al. (2017) in which only one sample is selected but reference conditions on the land surface are observed for the entire study period. Such an approach provides sample data for any point in time during the study period, which – in theory – allows for estimation of area for any time interval using a ratio estimator and indicator functions (Stehman, 2014). But as originally hypothesized, we found that only a few or no sample units at annual and bi-annual intervals were located in areas of the land change activities of interest, partly because of their very small area. As a result, several bi-annual estimates of *Forest-to-Pasture* and *Forest-to-Secondary Forest* were not significantly different from zero (i.e. area estimates had negative lower confidence bounds) or displayed large levels of uncertainty. The approach of using sample data representing each time interval generated more precise estimates but required examination of 1,050 sample units in each of the seven samples selected (i.e. $1,050 \times 7$ sample units). Even with such a large amount of sample data, some bi-annual area estimates of land change activities were not significantly different from zero. This finding is different from that of Cohen et al. (2016) and Potapov et al. (2017) who were able to use a single sample for annual estimation. However, the former study used a very large sample of 7,200 units, and the latter used only sample units mapped as forest cover loss for estimation of annual change dynamics, thus not including omissions of forest loss in the forest and non-forest strata, which, as evident by this study, often has a detrimental impact on precision of estimates. Still, the results presented here should not be taken as evidence that the single-sample-approach will not work for providing a

time series of estimates. Our result is just one example and others have already shown its utility (Potapov et al., 2017; Stehman 2014). As discussed further below, of importance to the lack of success of the single-sample-approach is the sheer size of the land categories of interest – even the most prevalent activity, Forest-to-Pasture, was just a tenth of a percent of the study area annually. In a situation where the area of the land change of interest is larger, as is often the case, we recommend an investigation into the feasibility of the single-sample-approach. Also, in a comparison of the margins of error between the approaches of single and multiple samples, the single-sample-approach yielded smaller errors for two out of seven years (Tables 6 and 7 in Appendix 3). With an increased focus on the reporting of activities at high temporal frequency, more research is needed to explore these types of approaches to inference of time series of area estimates.

Finally, a word about the issue of cost of sampling approaches discussed above. An underlying assumption of the discussion is that cost is synonymous with time and directly related to sample size. As a result, the single-sample-approach is assumed less costly simply because of the smaller sample size. But to use a single sample requires an assessment of land surface events over the entire estimation period (fifteen years in the case of the presented study). In rapidly changing landscapes, such an assessment would be time-consuming and could potentially eliminate the cost saving of the single-sample-approach.

5.2 Stratification and omission errors

An important difference between this study and Cohen et al. (2016) and Potapov et al. (2017) is the size of the land change activities of interest in relation to the study area. In the former studies, forest disturbance activities occupied 1.5-4.5% and 4-9% of the forest area per year respectively, whereas the corresponding numbers in this study are about a quarter of a percent. Inferring

information about such a small part of a population by sampling is difficult in general and often associated with large uncertainty; the same statistical problem is encountered in many medical and public health studies concerned with the prevalence of rare conditions, behaviors and diseases among large populations (Rahme & Joseph, 1998). In general, the problem is a consequence of the difficulty involved in achieving a sampling that results in sufficient precision in estimates of the phenomenon of interest (e.g. area of deforestation, prevalence of a disease, or votes in an election) across the entire population. In the context of using remote sensing to map and estimate areas of land change activities, a map depicting the spatial distribution of change is normally used to stratify the study area (i.e. the population) with the aim of ensuring sufficient sampling of activities. As witnessed in several countries, if very large strata are present, like *Forest* in this study, in which activities are observed (i.e. omission errors in the map used as stratification), the impact can be substantial (Espejo & Jonckheere 2017). From the formulas of the stratified estimator and the associated variance estimator (Cochran 1977, Eqs. 5.1 and 5.7), it can be deduced that the impact of omission errors is a result of the size of the stratum in which the errors occur in combination with the sampling intensity: the larger the stratum and the lower the sampling intensity, the higher the impact of omitted land change activity, especially if the activity data stratum is small. That is exactly the situation in this study: a land change activity stratum of less than a percent of the study area, and a forest stratum of 80% with low sampling intensity because of a relatively small sample size (less than 40%, or 400 out of 1,050, of the sampling units were allocated to the *Forest* stratum). By creating a buffer stratum around map classes of land change activity with a much smaller area but with higher sampling intensity that hopefully contains the activities omitted in the map, the impact of omission errors in the map is reduced. This approach has been successfully explored in other studies of land change activities

505in support of REDD+ (Potapov et al., 2017), and our results further support the recommendation
506of using a buffer stratum to reduce the impact of omission errors. The number and area weight of
507omission errors “captured” by the buffer stratum are presented in the confusion matrices in
508Appendix 2.

509 The issue of the impact of omission errors further highlights the importance of sample
510allocation when designing a stratified sample; a larger sample size in large strata will reduce the
511impact of omission errors (i.e. a sample allocated proportionally to the strata area) when
512sampling for area estimation (Stehman, 2012). As more and more countries and studies are
513facing issues related to omission errors and precision in estimates of land change activity data,
514combined with an increasing number of studies highlighting the efficiency of buffer strata, more
515research is needed on how to define buffer strata. For example, a larger buffer would capture
516more errors but its stratum weight would increase with its size; this in turn could be balanced by
517increased sampling intensity, but that would raise cost. How to best define the buffer spatially for
518optimal efficiency? These relevant questions require better answers if remote sensing is to reach
519its full potential for greenhouse gas reporting.

520 Stratified random sampling was used to select the location of the sample units for the
521single-sample- and multiple-sample-approach. The main benefit of using stratification when
522estimating land change is the ability to target the sampling to ensure a sample size in each
523category that is large enough to produce sufficiently precise area estimates (GFOI, 2016, p. 126).
524But for stratified sampling, achieving an allocation of sample units to strata that is proportional
525to the strata weights would require a very large sample size simply because some strata are very
526small. The result is often that fewer sample units are allocated to large strata relative their
527weights. As discussed above, the impact of omission errors is a result of the size of the stratum in

528which the errors occur in combination with the sampling intensity. Hence, in a situation as in this
529study with a very large forest stratum (90%) and very small land change stratum (<1%), simple
530random sampling merits consideration. The standard errors of the area estimates that would have
531occurred for simple random sampling were approximated by using the variance estimator for
532simple random sampling (Cochran 1977, p. 26) and the area proportions estimated from the
533stratified random sample (Table 5, Appendix 3). For the bi-annual area estimates of *Forest-to-*
534*Pasture*, the standard errors would have been two times larger on average if using simple random
535sampling instead of a stratified random sampling, and more than four times larger for certain
536intervals (although smaller than stratified random sampling for two out of the seven bi-annual
537estimates) -- hence, a substantial benefit was gained by the stratified design. The result supports
538the recommendations of Olofsson et al. (2014, p. 47) and GFOI (2016, p. 126) of employing a
539stratified design when aiming at estimating areas of land change activity.

540 Area estimates and the uncertainty in estimates are of primary importance to this study
541but because of the impact of omission errors on estimates, user's and producer's accuracy (Table
5423 and Table 4) of map classes need mentioning. The complement of omission error is producer's
543accuracy and for some of the map classes, especially the ones involving land change activities,
544large omission errors were observed as illustrated by the error matrices in Appendix 2. Look for
545example at the error matrices for 2001-2003 in Tables S1 and S2: even though 31 out of 50
546sample units allocated to the *Forest-to-Pasture* stratum were correct, the one single omission of
547*Forest-to-Pasture* in the *Forest* stratum represents an area of 114 Mha (or a 0.22 proportion of
548the study area)! In comparison, the 31 units correctly classified as *Forest-to-Pasture* represent an
549area of 40 Mha (0.077). The very large area proportion represented by this single omission error,
550in addition to a very low Producer's accuracy of 20.7% (Table 4), yields a large confidence

interval that includes zero (because the 2001-2003 estimate was not significantly different from zero, it was not plotted in Figure 7h). Note that the buffer stratum in this case “captures” 11 sample units observed as *Forest-to-Pasture* that otherwise would have been present in the *Forest* stratum to further decrease the precision of the area of *Forest-to-Pasture*. The total area represented by these 11 units was 20 Mha (0.037).

Finally, it is important to mention that the allocation of 50 units per rare stratum was chosen to balance the precision of area and accuracy estimates of these classes (Olofsson et al. 2014). However, if the only objective is to maximize the precision of area estimates, an allocation more heavily weighted to the largest class, in this case the *Forest* stratum, would be advisable.

5.3 Future steps

A major motivation for this study is to advance the monitoring of carbon dynamics associated with land change activities. We envision a system that tracks carbon emissions and removals in time and space simultaneously by coupling the presented methodology with a carbon bookkeeping model. Research is currently underway to implement a carbon bookkeeping model (Reinmann et al., 2016) “on top” of the presented monitoring system such that carbon dynamics are computed at the pixel level following land activities as informed by the CCDC/YATSM algorithm. A complicated but important component of such a framework will be estimation of bias and uncertainty. Most carbon bookkeeping models suitable for a gain/loss approach to estimating carbon emissions operate on estimates pertaining to large areas and large time spans (Houghton et al., 2012; Kuemmerle et al., 2011; Olofsson et al., 2011). For the modeling of carbon emissions to be spatially explicit, estimates of area bias and uncertainty at the population scale need to be spatialized, preferably at the pixel level. For example, a conversion of primary

574forest to pasture followed by regeneration of forest would trigger a release of carbon from the
575logged primary forest and soil according to the emissions curves used in the model, followed by
576sequestration of carbon by the recovering forest according to a pre-defined growth curve.
577Because such events would occur in one specific pixel, there is no direct way of knowing if the
578conversions are commission errors or actual events on land surface, even if population-specific
579estimates of bias and uncertainty exist. New and exciting research published recently attempts to
580predict the spatial variation in map accuracy down to the pixel-level using population-scale
581estimates of map accuracy and Landsat spectral features (Khatami et al., 2017a, 2017b). Such
582solutions could potentially provide pixel-level information that could be used to propagate bias
583and uncertainty information to estimates of carbon emission and removals. Another issue that
584requires attention is the carbon content (emissions factors) of landscapes experiencing recovery
585or degradation. While recent studies in the Amazon have started to provide such important data
586(Longo et al., 2016; Poorter et al., 2016), more measurements are needed to better understand the
587carbon dynamics of post-disturbance landscapes.

588 Finally, a note on forest degradation. Forest degradation is defined by the IPCC as the
589process leading to long-term loss of carbon but without a change in land cover (GFOI, 2016). We
590did not consider forest degradation but the IPCC definition and the monitoring approach
591presented provide an opportunity for future work to include degradation: as the trend in spectral
592signature is monitored, and land category labels are provided for each time series segment, a
593segment classified as *Forest* while also exhibiting a spectral trend indicative of vegetation loss
594(such as an increase in shortwave infrared or red surface reflectance) would represent potential
595forest degradation. Research is currently being conducted in tropical landscapes to characterize
596forest degradation by spectral signatures and CCDC/YATSM model coefficients.

5976. Conclusions

598The Colombian Amazon has experienced a continuous level of deforestation but at a small rate
599of less than 0.3% of the study area, or around 103 kha, for the 2013 – 2015 period. The
600deforestation, primarily driven by establishment of pasturelands, was estimated to have increased
601after 2005. Some of the post-deforestation landscapes did not stay deforested but were
602abandoned and reverted to secondary forest. We estimated that around 29 kha of the pasturelands
603were quickly abandoned in the 2013 – 2015 period, -- hence, less than the equivalent of 30% of
604the post-deforestation landscapes was estimated to have begun to regenerate. These results show
605that the fate of post-disturbance landscapes can be monitored and estimated with the presented
606methodology, but that more work is needed to further reduce the uncertainties. Increasing sample
607size, improving map accuracy and introducing buffer strata are all viable approaches to increase
608precision. The latter option was tested and it was found that the addition of a buffer stratum to
609capture omission errors had a marked effect on reducing the uncertainty on area estimates.
610Guidelines for how to design buffer strata in other situations with different distributions of strata
611weights, sample size, map accuracies etc. require more research. Finally, it was determined that
612the use of a single sample to estimate the area of land change activities at bi-annual frequency
613did not achieve acceptable levels of precision. Higher precision was achieved when sample data
614were collected for each time interval for which area estimates were desired.

615Acknowledgements

616This study was funded by NASA CMS grant NNX16AP26G (PI: Olofsson), SilvaCarbon
617Research grant 14-DG-11132762-347 (PI: Olofsson) and USGS/NASA Landsat Science Team

618grant (PI: Woodcock). We thank Chongyang Zhu, Katelyn Tarrio and Yihao Liu for assisting
619with the sample data collection. Their hard work and dedication are greatly appreciated.

620

621References

- 622Achard, F., Beuchle, R., Mayaux, P., Stibig, H.-J., Bodart, C., Brink, A., Carboni, S., Desclée,
623 B., Donnay, F., Eva, H.D., Lupi, A., Raši, R., Seliger, R., Simonetti, D., 2014.
624 Determination of tropical deforestation rates and related carbon losses from 1990 to
625 2010. *Glob. Change Biol.* 20, 2540–2554. <https://doi.org/10.1111/gcb.12605>
- 626Achard, F., Eva, H.D., Stibig, H.-J., Mayaux, P., Gallego, J., Richards, T., Malingreau, J.-P.,
627 2002. Determination of Deforestation Rates of the World's Humid Tropical Forests.
628 *Science* 297, 999–1002. <https://doi.org/10.1126/science.1070656>
- 629Aide, T.M., Clark, M.L., Grau, H.R., López-Carr, D., Levy, M.A., Redo, D., Bonilla-Moheno,
630 M., Riner, G., Andrade-Núñez, M.J., Muñiz, M., 2013. Deforestation and Reforestation
631 of Latin America and the Caribbean (2001–2010). *Biotropica* 45, 262–271.
632 <https://doi.org/10.1111/j.1744-7429.2012.00908.x>
- 633Armenteras, D., Rudas, G., Rodriguez, N., Sua, S., Romero, M., 2006. Patterns and causes of
634 deforestation in the Colombian Amazon. *Ecol. Indic.* 6, 353–368.
- 635Asner, G.P., Clark, J.K., Mascaro, J., Galindo García, G.A., Chadwick, K.D., Navarrete
636 Encinales, D.A., Paez-Acosta, G., Cabrera Montenegro, E., Kennedy-Bowdoin, T.,
637 Duque, á., Balaji, A., von Hildebrand, P., Maatoug, L., Phillips Bernal, J.F., Yepes
638 Quintero, A.P., Knapp, D.E., García Dávila, M.C., Jacobson, J., Ordóñez, M.F., 2012.
639 High-resolution mapping of forest carbon stocks in the Colombian Amazon.
640 *Biogeosciences* 9, 2683–2696. <https://doi.org/10.5194/bg-9-2683-2012>
- 641Baccini, A., Goetz, S.J., Walker, W.S., Laporte, N.T., Sun, M., Sulla-Menashe, D., Hackler, J.,
642 Beck, P.S.A., Dubayah, R., Friedl, M.A., Samanta, S., Houghton, R.A., 2012. Estimated
643 carbon dioxide emissions from tropical deforestation improved by carbon-density maps.
644 *Nat. Clim. Change* 2, 182–185. <https://doi.org/10.1038/nclimate1354>
- 645Baccini, A., Walker, W., Carvalho, L., Farina, M., Sulla-Menashe, D., Houghton, R.A., 2017.
646 Tropical forests are a net carbon source based on aboveground measurements of gain and
647 loss. *Science* eam5962. <https://doi.org/10.1126/science.eam5962>
- 648Breiman, L., 2001. Random Forests. *Mach. Learn.* 45, 5–32.
649 <https://doi.org/10.1023/A:1010933404324>
- 650Brown, S., 1997. Estimating biomass and biomass change of tropical forests: a primer, FAO
651 forestry paper. Food and Agriculture Organization of the United Nations, Rome.
- 652Cabrera, E., Vargas, D., Galindo, G., García, M.C., Ordoñez, M.F., Vergara, L., Pacheco, A.,
653 Rubiano, J., Giraldo, P., IDEAM, 2011. Memoria técnica de la cuantificación de la
654 deforestación histórica nacional – escalas gruesa y fina.
- 655Cochran, W.G., 1977. *Sampling Techniques*, 3rd Edition, 3rd edition. ed. John Wiley & Sons,
656 New York.
- 657Cohen, W.B., Yang, Z., Stehman, S.V., Schroeder, T.A., Bell, D.M., Masek, J.G., Huang, C.,
658 Meigs, G.W., 2016. Forest disturbance across the conterminous United States from 1985–
659 2012: The emerging dominance of forest decline. *For. Ecol. Manag., Special Section:*

660 Forest Management for Climate Change 360, 242–252.
 661 <https://doi.org/10.1016/j.foreco.2015.10.042>
 662 DeFries, R.S., Houghton, R.A., Hansen, M.C., Field, C.B., Skole, D., Townshend, J., 2002.
 663 Carbon emissions from tropical deforestation and regrowth based on satellite
 664 observations for the 1980s and 1990s. *Proc. Natl. Acad. Sci.* 99, 14256–14261.
 665 <https://doi.org/10.1073/pnas.182560099>
 666 Duivenvoorden, J.F., 1996. Patterns of Tree Species Richness in Rain Forests of the Middle
 667 Caqueta Area, Colombia, NW Amazonia. *Biotropica* 28, 142–158.
 668 <https://doi.org/10.2307/2389070>
 669 Espejo, A., Jonckheere, I., 2017. Proceedings: Technical Workshop on Lessons learned from
 670 Accuracy Assessments in the context of REDD+. FAO, Rome.
 671 Etter, A., McAlpine, C., Phinn, S., Pullar, D., Possingham, H., 2006a. Unplanned land clearing
 672 of Colombian rainforests: Spreading like disease? *Landsc. Urban Plan.* 77, 240–254.
 673 Etter, A., McAlpine, C., Wilson, K., Phinn, S., 2006b. Regional patterns of agricultural land use
 674 and deforestation in Colombia. *Agric. Ecosyst. Environ.* 114, 369–386. <https://doi.org/10.1016/j.agee.2005.11.013>
 675 <https://doi.org/10.1016/j.agee.2005.11.013>
 676 FAO, 2010. Global Forest Resources Assessment 2010. Food and Agriculture Organization of
 677 the United Nations, Rome.
 678 FAO (Ed.), 1993. Forest resources assessment 1990: tropical countries, FAO forestry paper.
 679 Food and Agriculture Organization of the United Nations, Rome.
 680 Galindo, G., Espejo, O., Ramirez, J., Forero, C., Valbuena, C., Rubiano, J., Lozano, R.,
 681 Vargas, K., Palacios, A., Palacios, S., Franco, C., Granados, E., Vergara, L., Cabrera,
 682 E., 2014. Memoria técnica de la Cuantificación de la superficie de bosque natural y
 683 deforestación a nivel nacional. Actualización Periodo 2012 – 2013. Bogota, D.C.
 684 Gebhardt, S., Wehrmann, T., Ruiz, M.A.M., Maeda, P., Bishop, J., Schramm, M., Kopeinig, R.,
 685 Cartus, O., Kellndorfer, J., Ressl, R., Santos, L.A., Schmidt, M., 2014. MAD-MEX:
 686 Automatic Wall-to-Wall Land Cover Monitoring for the Mexican REDD-MRV Program
 687 Using All Landsat Data. *Remote Sens.* 6, 3923–3943. <https://doi.org/10.3390/rs6053923>
 688 GFOI, 2016. Integrating remote-sensing and ground-based observations for estimation of
 689 emissions and removals of greenhouse gases in forests: Methods and Guidance from the
 690 Global Forest Observations Initiative., 2nd ed. Food and Agriculture Organization of the
 691 United Nations, Rome.
 692 GFOI, 2014. Integrating remote-sensing and ground-based observations for estimation of
 693 emissions and removals of greenhouse gases in forests: Methods and Guidance from the
 694 Global Forest Observations Initiative., 1st ed. Group on Earth Observations, Geneva.
 695 Goetz, S.J., Hansen, M., Houghton, R.A., Walker, W., Laporte, N., Busch, J., 2015.
 696 Measurement and monitoring needs, capabilities and potential for addressing reduced
 697 emissions from deforestation and forest degradation under REDD+. *Environ. Res. Lett.*
 698 10, 123001. <https://doi.org/10.1088/1748-9326/10/12/123001>
 699 Hansen, M.C., Potapov, P.V., Moore, R., Hancher, M., Turubanova, S.A., Tyukavina, A., Thau,
 700 D., Stehman, S.V., Goetz, S.J., Loveland, T.R., Kommareddy, A., Egorov, A., Chini, L.,
 701 Justice, C.O., Townshend, J.R.G., 2013. High-Resolution Global Maps of 21st-Century
 702 Forest Cover Change. *Science* 342, 850–853. <https://doi.org/10.1126/science.1244693>
 703 Harris, N.L., Brown, S., Hagen, S.C., Saatchi, S.S., Petrova, S., Salas, W., Hansen, M.C.,
 704 Potapov, P.V., Lotsch, A., 2012. Baseline Map of Carbon Emissions from Deforestation
 705 in Tropical Regions. *Science* 336, 1573–1576. <https://doi.org/10.1126/science.1217962>

706 Holden, C., 2016a. yatsm: Yet Another Time Series Model (YATSM): v0.6.1.
 707 <https://doi.org/10.5281/zenodo.51336>
 708 Holden, C., 2016b. TSTools: TSTools: v1.1.1. <https://doi.org/10.5281/zenodo.55045>
 709 Houghton, R.A., House, J.I., Pongratz, J., van der Werf, G.R., DeFries, R.S., Hansen, M.C., Le
 710 Quéré, C., Ramankutty, N., 2012. Carbon emissions from land use and land-cover
 711 change. *Biogeosciences* 9, 5125–5142. <https://doi.org/10.5194/bg-9-5125-2012>
 712 IDEAM, 2016. Sexto Boletín de Alertas Tempranas de Deforestación (AT-D). Segundo semestre
 713 2015.
 714 Instituto Nacional de Pesquisas Espaciais (INPE), 2016. Deforestation estimates in the Brazilian
 715 Amazon [WWW Document]. URL <http://www.obt.inpe.br/prodes/index.php> (accessed
 716 8.29.16).
 717 IPCC, 2006. 2006 IPCC guidelines for national greenhouse gas inventories.
 718 IPCC, 2003. Good practice guidance for land use, land-use change and forestry.
 719 Kennedy, R.E., Yang, Z., Cohen, W.B., 2010. Detecting trends in forest disturbance and
 720 recovery using yearly Landsat time series: 1. LandTrendr — Temporal segmentation
 721 algorithms. *Remote Sens. Environ.* 114, 2897–2910.
 722 <https://doi.org/10.1016/j.rse.2010.07.008>
 723 Khatami, R., Mountrakis, G., Stehman, S.V., 2017a. Mapping per-pixel predicted accuracy of
 724 classified remote sensing images. *Remote Sens. Environ.* 191, 156–167.
 725 <https://doi.org/10.1016/j.rse.2017.01.025>
 726 Khatami, R., Mountrakis, G., Stehman, S.V., 2017b. Predicting individual pixel error in remote
 727 sensing soft classification. *Remote Sens. Environ.* 199, 401–414.
 728 <https://doi.org/10.1016/j.rse.2017.07.028>
 729 Kim, O.S., 2010. An Assessment of Deforestation Models for Reducing Emissions from
 730 Deforestation and Forest Degradation (REDD). *Trans. GIS* 14, 631–654.
 731 <https://doi.org/10.1111/j.1467-9671.2010.01227.x>
 732 Kuemmerle, T., Olofsson, P., Chaskovskyy, O., Baumann, M., Ostapowicz, K., Woodcock, C.E.,
 733 Houghton, R.A., Hostert, P., Keeton, W.S., Radeloff, V.C., 2011. Post-Soviet farmland
 734 abandonment, forest recovery, and carbon sequestration in western Ukraine. *Glob.*
 735 *Change Biol.* 17, 1335–1349. <https://doi.org/10.1111/j.1365-2486.2010.02333.x>
 736 Longo, M., Keller, M.M., dos-Santos, M.N., Leitold, V., Pinagé, E.R., Baccini, A., Saatchi, S.,
 737 Nogueira, E.M., Batistella, M., Morton, D.C., 2016. Aboveground biomass variability
 738 across intact and degraded forests in the Brazilian Amazon. *Glob. Biogeochem. Cycles*
 739 2016GB005465. <https://doi.org/10.1002/2016GB005465>
 740 McRoberts, R.E., 2011. Satellite image-based maps: Scientific inference or pretty pictures?
 741 *Remote Sens. Environ.* 115, 715–724. <https://doi.org/10.1016/j.rse.2010.10.013>
 742 Olofsson, P., Foody, G.M., Herold, M., Stehman, S.V., Woodcock, C.E., Wulder, M.A., 2014.
 743 Good practices for estimating area and assessing accuracy of land change. *Remote Sens.*
 744 *Environ.* 148, 42–57. <https://doi.org/10.1016/j.rse.2014.02.015>
 745 Olofsson, P., Foody, G.M., Stehman, S.V., Woodcock, C.E., 2013. Making better use of
 746 accuracy data in land change studies: Estimating accuracy and area and quantifying
 747 uncertainty using stratified estimation. *Remote Sens. Environ.* 129, 122–131.
 748 <https://doi.org/10.1016/j.rse.2012.10.031>
 749 Olofsson, P., Kuemmerle, T., Griffiths, P., Knorn, J., Baccini, A., Gancz, V., Blujdea, V.,
 750 Houghton, R.A., Abrudan, I.V., Woodcock, C.E., 2011. Carbon implications of forest

751 restitution in post-socialist Romania. *Environ. Res. Lett.* 6, 045202.
752 <https://doi.org/10.1088/1748-9326/6/4/045202>

753 Olson, D.M., Dinerstein, E., 2002. The Global 200: Priority Ecoregions for Global Conservation.
754 *Ann. Mo. Bot. Gard.* 89, 199–224. <https://doi.org/10.2307/3298564>

755 Orme, C.D.L., Davies, R.G., Burgess, M., Eigenbrod, F., Pickup, N., Olson, V.A., Webster, A.J.,
756 Ding, T.-S., Rasmussen, P.C., Ridgely, R.S., Stattersfield, A.J., Bennett, P.M.,
757 Blackburn, T.M., Gaston, K.J., Owens, I.P.F., 2005. Global hotspots of species richness
758 are not congruent with endemism or threat. *Nature* 436, 1016–1019.
759 <https://doi.org/10.1038/nature03850>

760 Poorter, L., Bongers, F., Aide, T.M., Almeyda Zambrano, A.M., Balvanera, P., Becknell, J.M.,
761 Boukili, V., Brancalion, P.H.S., Broadbent, E.N., Chazdon, R.L., Craven, D., de
762 Almeida-Cortez, J.S., Cabral, G.A.L., de Jong, B.H.J., Denslow, J.S., Dent, D.H.,
763 DeWalt, S.J., Dupuy, J.M., Durán, S.M., Espírito-Santo, M.M., Fandino, M.C., César,
764 R.G., Hall, J.S., Hernandez-Stefanoni, J.L., Jakovac, C.C., Junqueira, A.B., Kennard, D.,
765 Letcher, S.G., Licona, J.-C., Lohbeck, M., Marín-Spiotta, E., Martínez-Ramos, M.,
766 Massoca, P., Meave, J.A., Mesquita, R., Mora, F., Muñoz, R., Muscarella, R., Nunes,
767 Y.R.F., Ochoa-Gaona, S., de Oliveira, A.A., Orihuela-Belmonte, E., Peña-Claros, M.,
768 Pérez-García, E.A., Piotto, D., Powers, J.S., Rodríguez-Velázquez, J., Romero-Pérez,
769 I.E., Ruíz, J., Saldarriaga, J.G., Sanchez-Azofeifa, A., Schwartz, N.B., Steininger, M.K.,
770 Swenson, N.G., Toledo, M., Uriarte, M., van Breugel, M., van der Wal, H., Veloso,
771 M.D.M., Vester, H.F.M., Vicentini, A., Vieira, I.C.G., Bentos, T.V., Williamson, G.B.,
772 Rozendaal, D.M.A., 2016. Biomass resilience of Neotropical secondary forests. *Nature*
773 530, 211–214. <https://doi.org/10.1038/nature16512>

774 Potapov, P.V., Dempewolf, J., Talero, Y., Hansen, M.C., Stehman, S.V., Vargas, C., Rojas, E.J.,
775 Castillo, D., Mendoza, E., A Calderón, Giudice, R., Malaga, N., Zutta, B.R., 2014.
776 National satellite-based humid tropical forest change assessment in Peru in support of
777 REDD+ implementation. *Environ. Res. Lett.* 9, 124012. [https://doi.org/10.1088/1748-](https://doi.org/10.1088/1748-9326/9/12/124012)
778 [9326/9/12/124012](https://doi.org/10.1088/1748-9326/9/12/124012)

779 Potapov, P., Siddiqui, B.N., Iqbal, Z., Aziz, T., Zzaman, B., Islam, A., Pickens, A., Talero, Y.,
780 Tyukavina, A., Turubanova, S., Hansen, M.C., 2017. Comprehensive monitoring of
781 Bangladesh tree cover inside and outside of forests, 2000–2014. *Environ. Res. Lett.* 12,
782 104015. <https://doi.org/10.1088/1748-9326/aa84bb>

783 QGIS Development Team, 2009. QGIS Geographic Information System. Open Source
784 Geospatial Foundation.

785 Rahme, E., Joseph, L., 1998. Estimating the prevalence of a rare disease: adjusted maximum
786 likelihood. *Journal of the Royal Statistical Society: Series D (The Statistician)* 47, 149–
787 158. <https://doi.org/10.1111/1467-9884.00120>

788 Reinmann, A.B., Hutyrá, L.R., Trlica, A., Olofsson, P., 2016. Assessing the global warming
789 potential of human settlement expansion in a mesic temperate landscape from 2005 to
790 2050. *Sci. Total Environ.* 545–546, 512–524.
791 <https://doi.org/10.1016/j.scitotenv.2015.12.033>

792 Sánchez-Cuervo, A.M., Aide, T.M., Clark, M.L., Etter, A., 2012. Land Cover Change in
793 Colombia: Surprising Forest Recovery Trends between 2001 and 2010. *PLOS ONE* 7,
794 e43943. <https://doi.org/10.1371/journal.pone.0043943>

795Stehman, S.V., 2014. Estimating area and map accuracy for stratified random sampling when the
796 strata are different from the map classes. *Int. J. Remote Sens.* 35, 4923–4939.
797 <https://doi.org/10.1080/01431161.2014.930207>

798Stehman, S.V., 2013. Estimating area from an accuracy assessment error matrix. *Remote Sens.*
799 *Environ.* 132, 202–211. <https://doi.org/10.1016/j.rse.2013.01.016>

800Stehman, S.V., 2012. Impact of sample size allocation when using stratified random sampling to
801 estimate accuracy and area of land-cover change. *Remote Sens. Lett.* 3, 111–120. <https://doi.org/10.1080/01431161.2010.541950>

803Stehman, S.V., 2000. Practical Implications of Design-Based Sampling Inference for Thematic
804 Map Accuracy Assessment. *Remote Sens. Environ.* 72, 35–45.
805 [https://doi.org/10.1016/S0034-4257\(99\)00090-5](https://doi.org/10.1016/S0034-4257(99)00090-5)

806Sy, V.D., Herold, M., Achard, F., Beuchle, R., Clevers, J.G.P.W., Lindquist, E., Verchot, L.,
807 2015. Land use patterns and related carbon losses following deforestation in South
808 America. *Environ. Res. Lett.* 10, 124004. [https://doi.org/10.1088/1748-](https://doi.org/10.1088/1748-9326/10/12/124004)
809 [9326/10/12/124004](https://doi.org/10.1088/1748-9326/10/12/124004)

810UNFCCC, 2018. FOCUS: Mitigation - Reporting on national implementation and MRV |
811 UNFCCC [WWW Document]. URL
812 <https://unfccc.int/topics/mitigation/workstreams/measurement--reporting-and-verification>
813 (accessed 10.9.18).

814UNODC, 2016. Monitoreo de territorios afectados por cultivos ilícitos 2015. Government of
815 Colombia/United Nations Office on Drugs and Crime., Bogotá.

816UN-REDD, 2016. UN-REDD Programme [WWW Document]. UN-REDD Programme. URL
817 <http://www.un-redd.org/> (accessed 7.25.16).

818USGS, 2010. ESPA [WWW Document]. URL <http://espa.cr.usgs.gov/index/> (accessed 7.26.16).

819Verbesselt, J., Hyndman, R., Newnham, G., Culvenor, D., 2010. Detecting trend and seasonal
820 changes in satellite image time series. *Remote Sens. Environ.* 114, 106–115.
821 <https://doi.org/10.1016/j.rse.2009.08.014>

822Woodcock, C.E., Allen, R., Anderson, M., Belward, A., Bindschadler, R., Cohen, W., Gao, F.,
823 Goward, S.N., Helder, D., Helmer, E., Nemani, R., Oreopoulos, L., Schott, J.,
824 Thenkabail, P.S., Vermote, E.F., Vogelmann, J., Wulder, M.A., Wynne, R., 2008. Free
825 Access to Landsat Imagery. *Science* 320, 1011–1011.
826 <https://doi.org/10.1126/science.320.5879.1011a>

827Zhu, Z., Woodcock, C.E., 2012. Object-based cloud and cloud shadow detection in Landsat
828 imagery. *Remote Sensing of Environment* 118, 83–94.
829 <https://doi.org/10.1016/j.rse.2011.10.028>

830Zhu, Z., Woodcock, C.E., 2014a. Continuous change detection and classification of land cover
831 using all available Landsat data. *Remote Sens. Environ.* 144, 152–171.
832 <https://doi.org/10.1016/j.rse.2014.01.011>

833Zhu, Z., Woodcock, C.E., 2014b. Automated cloud, cloud shadow, and snow detection in
834 multitemporal Landsat data: An algorithm designed specifically for monitoring land
835 cover change. *Remote Sensing of Environment* 152, 217–234.
836 <https://doi.org/10.1016/j.rse.2014.06.012>

837Zhu, Z., Woodcock, C.E., Olofsson, P., 2012. Continuous monitoring of forest disturbance using all available Landsat imagery. *Remote*
838 *Sens. Environ.*, Landsat Legacy Special Issue 122, 75–91.
839 <https://doi.org/10.1016/j.rse.2011.10.030>

841

842List of figure captions

843- Figure 1. Study area and Landsat scenes processed. The Landsat WRS-2 path and row are
844displayed for each scene.

845- Figure 2. Time series of short-wave infrared observations (the SWIR1 band) acquired by
846Landsat -5, -7 and -8 of a pasture in the Colombian Amazon. A clear gap in available
847observations can be seen between 1992 and 1997. Landsat WRS-2 path 7, row 59; coordinates
84873.9290 W, 1.9687 N.

849- Figure 3. Time series of observations of SWIR1 surface reflectance measured by Landsat
850TM, ETM+, OLI band 5 (blue dots; upper) and snippets of Landsat composites in NIR-SWIR1-
851RED band combination (lower). CCDC predictions of surface reflectance are plotted as solid
852lines and detected breaks as thick red circles. (Landsat path-row 6-59, pixel coordinates: 72.1795
853W, 1.4725 N).

854- Figure 4. Overview of the workflow used to estimate areas, accuracies and uncertainty
855using maps created from time series of Landsat imagery as a source of stratification and
856manually collected reference data.

857- Figure 5. Examples of stable forest in time series of Landsat SWIR1 surface reflectance
858for a pixel in a) an area of intact primary forest, b) the edge between forest and shrublands and c)
859a riparian forest next to natural grasslands. Landsat subsets in RGB NIR-SWIR1-RED band
860combination are shown for dates near the beginning and end of the time series, respectively.
861High-resolution imagery (zoomed) of the example pixels from Bing Maps are shown to the right
862of the Landsat images.

863- Figure 6. Map of IPCC land categories including conversions between 2001 and 2016
864detailing: A) areas of conversion from forest to pasture, and B) areas with evidence of secondary
865forest and heterogeneous land changes.

866- Figure 7. Bi-annual area estimates with 95% confidence intervals (dashed lines) for stable
867and change classes, estimated from the reference data using the multiple-samples-approach.
868Cross markers represent values that are statistically different from zero (i.e. confidence interval
869does not include zero). The red continuous line represent areas obtained directly from the map by
870pixel-counting. The years on the x-axes represent the middle of each bi-annual period for
871visualization purposes (02 for 2002, 04 for 2004 and so on). The y-axes were set independently
872to aid in the visualization of the areas (but kept similar in rows where the same scale was
873sensible) given the large differences in magnitude. The panel for the “Other-to-other” class was
874removed, as it did not contain any relevant information.

875- Figure 8. Comparison of margins of error of the bi-annual Forest-to-Pasture area
876estimates obtained by multiple-samples-approach (*with the Buffer stratum*) and single-sample-
877approach.

878

879